Level anticrossing effect on electron properties of coupled quantum wells under an in-plane magnetic field

A. Hernández-Cabrera* and P. Aceituno
Departamento de Física Básica, Universidad de La Laguna, 38206 La Laguna, Tenerife, Spain

F. T. Vasko
Institute of Semiconductor Physics, NAS Ukraine, Pr. Nauki 45, Kiev, 252650, Ukraine
(Received 22 March 1999)

The influence of an in-plane magnetic field on the energy spectrum and zero-temperature equilibrium properties of tunnel-coupled double and triple quantum wells is studied. Both the appearance of the gap due to anticrossing of two energy branches and the peculiarities of the third-order crossing point (for symmetric triple quantum well case) are discussed. As results, magnetization of two-dimensional electrons in double and triple quantum wells is modified essentially if the Fermi level is localized near such peculiarities. Another effect under consideration is the interlevel charge redistribution between quantum wells and the transverse voltage induced by the in-plane magnetic field. Self-consistent numerical calculations for double and triple quantum wells, which take into account the modifications of energy spectra under gate voltage, are presented. [S0163-1829(99)09431-X]

I. INTRODUCTION

Currently noticeable interest is focused on the electronic properties of double and triple quantum wells (DQW's and TQW's) and on the transport (or optical) phenomena in such semiconductor structures. Such tunnel-coupled two-dimensional (2D) electron systems, when subjected to a perpendicular or parallel (in-plane) magnetic field, exhibit a set of new physical phenomena. While the effect of a perpendicular magnetic field is due to Landau quantization, the influence of an in-plane magnetic field appears due to different displacements of the energy dispersion parabolas of the different quantum wells (QW's). The sketches of the energy spectrum modifications under an in-plane magnetic field are shown in Fig. 1. It is clear that different types of cross points between dispersion parabolas (which are independent for tunnel-uncoupled wells) are possible for DQW's and TQW's the type of peculiarity is determined both by the strength of the magnetic field H and by the parameters of the tunnel-coupled structure.

Such in-plane magnetic-field-induced modifications of the energy spectra in DQW's and TQW's change the in-plane conductivity of these systems (see experimental data for DQW's in Refs. 1–6 and first measurements for TQW's in Ref. 7; theoretical results for DQW's are discussed in Ref. 8) and the photoluminescence spectra.[9] Two reasons for conductivity changes were found: the modification of the resistance resonance peak (these results are reviewed in Ref. 10) and the formation of density of states singularity[11] due to the anticrossing effect presented in Figs. 1(b) and 1(d). The photoluminescence line shape depends on the modification of hole states and is due to the many-particle interaction.[12] In the recent years, a weak perpendicular magnetic field has been employed as a probe in order to study the effects of in-plane field on tunnel-coupled states of electrons (Shubnikov—de Haas oscillations[5] and cyclotron resonance absorption[13] have been measured). Note that all aforementioned papers deal with the transport properties when the peculiarities of the energy spectra together with other factors (scattering processes, transformation of the hole states) are essentials. The aim of this paper is the description of the *equilibrium* electron properties of tunnel coupled structures when collisions do not determine the character of the response. Both the magnetization of tunnel-coupled QW's under in-plane field and magnetoinduced transverse voltage allow the direct (collisionless) investigation of the energy spectrum peculiarities.

Our calculations are based on the one-electron Hamiltonian for the usual effective mass approximation

$$\overline{H}=\frac{[\mathbf{p}-e\mathbf{A}(z)/c]^2}{2m}-\frac{\hbar^2}{2m}\frac{d^2}{dz^2}+U_{\mathrm{CQW}}(z)+U_{\mathrm{sc}}(z) \quad (1)$$

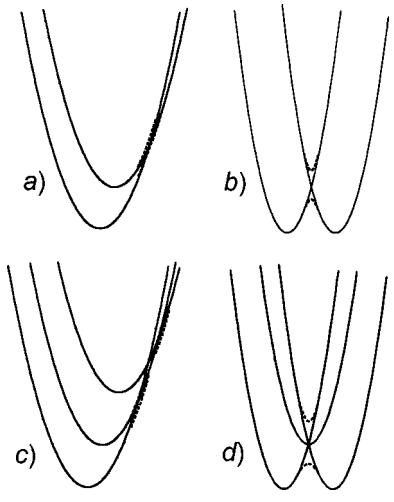

FIG. 1. Sketches of the energy spectra of symmetric tunnel-coupled QW showing the types of cross-points: (a) ''vertical'' crossing in DQW's; (b) ''horizontal'' crossing in DQW's; (c) two ''vertical'' cross points for TQW's; (d) triple-cross point in TQW's. The anticrossing effect is shown by the dashed lines.

Here, $\mathbf{p}$ is the 2D momentum, $\mathbf{A}(z)$ is the vector potential corresponding to the in-plane magnetic field $\mathbf{H}$ (below $\mathbf{H}\|OY$), $U_{\mathrm{CQW}}(z)$ is the confinement potential of the heterostructure along the z direction, which includes the transverse electric field, $F_{\perp}$, and $U_{\mathrm{sc}}(z)$ is the self-consistent Hartree potential, which is determined from the Poisson equation. In Sec. II, we use the tunneling approximation (which takes into account two or three tunnel-coupled levels only) for the consideration of the energy spectrum peculiarities; then we compare these results with the self-consistent numerical solutions of the eigenstate problem for the energy spectra of DQW's and TQW's. In the Sec. III, we present the analysis of the magnetization M and of the magnetoinduced transverse voltage δU; also, self-consistent results for the equilibrium quantities M and δU are presented. Discussion of our assumptions and concluding remarks are given in the last section.

II. ELECTRON ENERGY SPECTRUM

To consider the electron properties of tunnel-coupled DQW's and TQW's under in-plane magnetic field, we describe in this section the energy spectrum for these systems using both the simple analytic and the self-consistent numerical procedure. For the analytical consideration below we employ a basis of the electron ground states, which are described by the single well orbitals φ_{kz} for left (l-) and right (r-) wells of DQW's or l-, r-, and central (c-) wells for TQW's. In the framework of such approximation we will search for the solution of the eigenstate problem $\hat{H}\Psi = E\Psi$ in the form

$$\Psi(\mathbf{p},z) = \sum_k \psi_k(\mathbf{p})\varphi_{kz}, \tag{2}$$

where $k = l,r$ for DQW's or $k = l,c,r$ for TQW's. In the introduced basis, the columns $\psi_k(\mathbf{p})$ are determined from the eigenstate problem with the matrix Hamiltonian (we write here 3×3 matrix for the TQW's case)

$$\begin{vmatrix} \varepsilon_l(\mathbf{p}) & T_l & 0 \\ T_l & \varepsilon_c(\mathbf{p}) & T_r \\ 0 & T_r & \varepsilon_r(\mathbf{p}) \end{vmatrix}, \tag{3}$$

where T_l and T_r are the tunneling-matrix elements for l and r barriers, $\varepsilon_k(\mathbf{p})$ are the electronic dispersion laws for single kth QW under in-plane magnetic field:

$$\varepsilon_k(\mathbf{p}) = \varepsilon_{kH} + \frac{(p_x + mv_k)^2 + p_y^2}{2m}, \quad v_k = \frac{|e|H}{mc}(z_k - z_0), \tag{4}$$

and the characteristic velocities, v_k, contain an arbitrary coordinate z_0 due to the gauge invariance. The kth level energy ε_{kH} is introduced here as

$$\varepsilon_{kH} = \varepsilon_k + \frac{(eH/c)^2}{2m}\int dz\,\varphi_{kz}^2(z^2 - z_k^2), \tag{5}$$

where the proportional to H^2 intrawell corrections are usually negligible[8] and we use $\varepsilon_{kH} \sim \varepsilon_k$ below. The corresponding 2×2 matrix for DQW's contains single tunnel-matrix element T and was presented in Ref. 8. Thus, simple analytical consideration of the second or third order dispersion algebraic equations (for the DQW's or TQW's cases, correspondingly) permits us to analyze the energy spectra peculiarities.

The explicit expressions for $\pm$ branches of energy spectra in the DQW's structure case take the form

$$E_{\pm}(\mathbf{p}) = \frac{p^2}{2m} \pm \frac{\Delta_T(p_x)}{2},$$

$$\Delta_T(p_x) = \sqrt{(\Delta - v_H p_x)^2 + (2T)^2}, \tag{6}$$

where $v_r = -v_l \equiv v_H$ and $\Delta = \varepsilon_l - \varepsilon_r$ is the level splitting without tunneling. The equation $\partial E_{\pm}(\mathbf{p})/\partial p_x = 0$ gives us both the minimum energies for $\pm$ branches of spectra and the condition for transformation of the anticrossing structure from the ''vertical'' case [Fig. 1(a)] to the ''horizontal'' case with two additional extrema [Fig. 1(b)]. The last case causes the logarithmically divergent density of states,[11] which leads to the peculiarities of thermodynamic characteristics when the Fermi level intersects the horizontal anticrossing region. For the tunnel-uncoupled DQW's (with $T \to 0$) the minimal energies $\pm\Delta/2$ correspond to the momentum $\pm m v_H$ and the cross point is realized at $\overline{p_x} = \Delta/v_H$ (there are no anticrossing effect or logarithmic peculiarity of the density of states under such simplification).

For the TQW case we have to solve the cubic dispersion equation

$$(\varepsilon_{lp_x} - \xi)(\varepsilon_{cp_x} - \xi)(\varepsilon_{rp_x} - \xi) - T_r^2(\varepsilon_{lp_x} - \xi) - T_l^2(\varepsilon_{rp_x} - \xi) = 0, \tag{7}$$

where $\xi = E - p_y^2/(2m)$ includes the motion along the magnetic field. For the tunnel-uncoupled TQW's (with $T_{r,l} \to 0$) the triple-cross point could be realized at $\overline{p_x}$, which is determined from the conditions $\varepsilon_{l\overline{p_x}} = \varepsilon_{c\overline{p_x}} = \varepsilon_{r\overline{p_x}}$. Choosing $z_0 = z_c$, counting the energy from $\varepsilon_c = 0$, and using $\varepsilon_{cp_x} = p_x^2/(2m)$ these equations are transformed to $\varepsilon_l + v_l\overline{p_x} = \varepsilon_r + v_r\overline{p_x} = 0$. There is no solution for the general case (with $\varepsilon_l/\varepsilon_r \neq v_l/v_r$) and peculiarities of the energy spectra and of the density of states appear in the weak tunnel-coupled TQW's due to the contributions from two double-cross points between different branches of spectra (see above discussion for the DQW's case).

The triple-cross point occurs for the special case of the tunnel-uncoupled TQW's with $\varepsilon_l/\varepsilon_r = v_l/v_r$. For the tunnel-coupled TQW's case with $T_l \simeq T_r \equiv T$ (otherwise TQW's transforms to DQW's with additional uncoupled well) and $v_l \simeq -v_r \equiv v_H$ (so that $\varepsilon_l \simeq -\varepsilon_r \equiv \Delta/2$) we obtain the dispersion equation:

$$\left(\frac{p_x^2}{2m} - \xi\right)\left[\left(\frac{p_x^2}{2m} - \xi\right)^2 - \left(\frac{\Delta}{2} + v_H p_x\right)^2\right] - 2T^2\left(\frac{p_x^2}{2m} - \xi\right) = 0, \tag{8}$$

As a result, the triple-cross point is formed as the superposition of the horizontal anticrossing solutions, which are distinct from the DQW's case due to the larger tunnel-matrix element $\sqrt{2}T$, and to the simple parabolic branch inside the anticrossing gap [see Fig. 1(d)].

The self-consistent numerical procedure for the Schrödinger equation with the Hamiltonian (1) involves the Hartree potential, which is obtained from the Poisson equation in the following form:

$$U_{sc}(z)=\frac{4\pi e^2}{\varepsilon}\int_{-\infty}^{z}dz'(z-z')[n_D(z')-n_e(z')]. \quad (9)$$

Here $n_D(z)$ is the 3D concentration of donors, which we assume as a δ doping in the center of the heterostructure; ε is the dielectric permittivity, which is supposed to be uniform across heterostructure, and the 3D electron concentration, $n_e(z)$, is introduced in the usual way for the zero-temperature case with the Fermi energy ε_F:

$$n_e(z)=2\sum_j \int \frac{d\mathbf{p}}{(2\pi\hbar)^2}|\Psi_j(\mathbf{p}z)|^2\theta[\varepsilon_F-E_j(\mathbf{p})]$$

$$=\frac{2\rho_{2D}}{\pi}\sum_j \int dp_x|\Psi_{jp_x}(z)|^2\sqrt{\frac{\varepsilon_F-E_{jp_x}}{2m}}. \quad (10)$$

In the right-hand side of this equation we used the jth branch of the electron dispersion laws for DQW's or TQW's, $E_j(\mathbf{p})=E_{jp_x}+p_y^2/(2m)$, and performed the integration over p_y; ρ_{2D} is the 2D density of states. The Fermi energy, ε_F, in Eq. (10), is expressed through the total 2D electron density, n_e, according to

$$n_e=\frac{2\rho_{2D}}{\pi}\sum_j \int dp_x\sqrt{\frac{\varepsilon_F-E_{jp_x}}{2m}}, \quad (11)$$

and ε_F depends on H for the case of fixed concentration.

To numerically calculate the dispersion relations, i.e., the eigenvalues for different p_x values, we assume a flat-band approximation for the effective potential of the structure, as a first step of calculation. Then, we divide each quantum well and barrier potential in N_i rectangular pieces with a σ_i width. When $N_i\to\infty$, $\sigma_i\to 0$ and we reproduce the actual QW structure. In this case, we can use plane waves in each N_i part of the wells and barriers. The next step consists in applying the boundary conditions at each virtual interface, to say the continuity of $[1/m(z)\psi](\partial\psi/\partial z)$ [here we use the position-dependent effective mass $m(z)$]. We have done this self-consistently by using the transfer-matrix method together with the Hartree potential $U_{sc}(z)$. The transmission probability and energy levels are now obtained from $M_{22}=0$, M_{ij} being the matrix elements resulting from the matching of the boundaries between all pairs of virtual layers

$$M=[S^b(z_1)]^{-1}[S^w(z_1)][S^w(z_2)]^{-1}[S^b(z_2)]\ldots, \quad (12)$$

where

$$S^{w,b}(z)=\begin{pmatrix} \varphi_1^{w,b}(z) & \varphi_2^{w,b}(z) \\ \frac{\partial}{m(z)\partial z}\varphi_1^{w,b}(z) & \frac{\partial}{m(z)\partial z}\varphi_2^{w,b}(z)\end{pmatrix}, \quad (13)$$

and $\varphi_{1,2}^{w,b}(z)$ are the plane waves for wells (w) and barriers (b), respectively. Subindexes 1 and 2 indicate the two associate solutions of any second-order differential equation, as Eq. (1) is. Thus, for a given p_x value we obtain the different eigenvalues E_{jp_x} (see reference[14] for a more detailed description of the method).

Below, we present results of numerical calculations concerning the electron dispersion laws, E_{jp_x}, in DQW's and TQW's under in-plane magnetic field. We consider the $GaAs/Ga_{0.65}Al_{0.35}As$-based structures with a conduction-band offset of 300 meV, $m_{GaAs}=0.067m_e$, $m_{Ga_{0.65}Al_{0.35}As}=0.073m_e$. We have used two 70-Å well widths ($d_l=d_r$) for the DQW's case, separated by a 40-Å barrier width. The TQW consists on three wells, $d_l=d_r=d_c=70$ Å, with two 40-Å barrier widths. We have used a 2D carrier density of $3.10^{11}\,cm^{-2}$ for all cases. Fermi level depends on H through the dispersion relations and on the carrier density [see Eq. (11)]. We will restrict ourselves to symmetric QW's with and without external electric fields.

Results for self-consistent calculations of dispersion laws for symmetric DQW's and TQW's are presented in Figs. 2 and 3, respectively. The magnetic field produces different horizontal shifts of parabolas in the p_x direction and, then, they intersect themselves [Figs. 2(a) and 3(a)]. A partial energy gap results as these parabolas anticross. In addition, the electric field causes a disalignment of parabolas [see Figs. 2(b) and 3(b)] due to the additional contribution of the field energy. As a consequence, one can conclude from figures that vertical cross points only exist when the electric field is present. Also, vertical cross points can be found for asymmetric quantum wells with and without electric field.[14]

III. MAGNETIZATION AND INDUCED VOLTAGE

The above-described modifications of the energy spectra causes the changing of thermodynamic relations for tunnel-coupled structures under an in-plane magnetic field; in this section, we present the general expressions for the magnetization M and the induced voltage δU the discussions for the simplest case of weak tunnel-coupled structures, and the numerical results for DQW and TQW with the above-listed parameters. Both experimental and theoretical considerations of M have been done in the past for the case of transverse magnetic field applied to a single quantum well (QW) (see references and last results in Refs. 15 and 16). In such a case, the effect appears due to Landau quantization while for the case of in-plane magnetic field under study, M is due to the modifications of energy spectra, which are weak for single QW, leading to small values of M. These modifications lead also to the small transverse voltage induced by in-plane field, which have been calculated in Ref. 17 for the single QW case. However, for tunnel-coupled heterostructures, the effect of an in-plane magnetic field on thermodynamic quantities is significant when $\hbar\omega_c Z/\lambda_F$ (ω_c is the cyclotron frequency, Z is the interwell distance, and λ_F is the Fermi wavelength) is comparable to the level splitting energy [Δ_T in Eq. (6)].

The following analysis of the magnetization is based on the general expression for $M=-dE_e/dH$ as the first derivative of the electron energy per unit area, E_e. For the zero-temperature case under consideration E_e takes the form

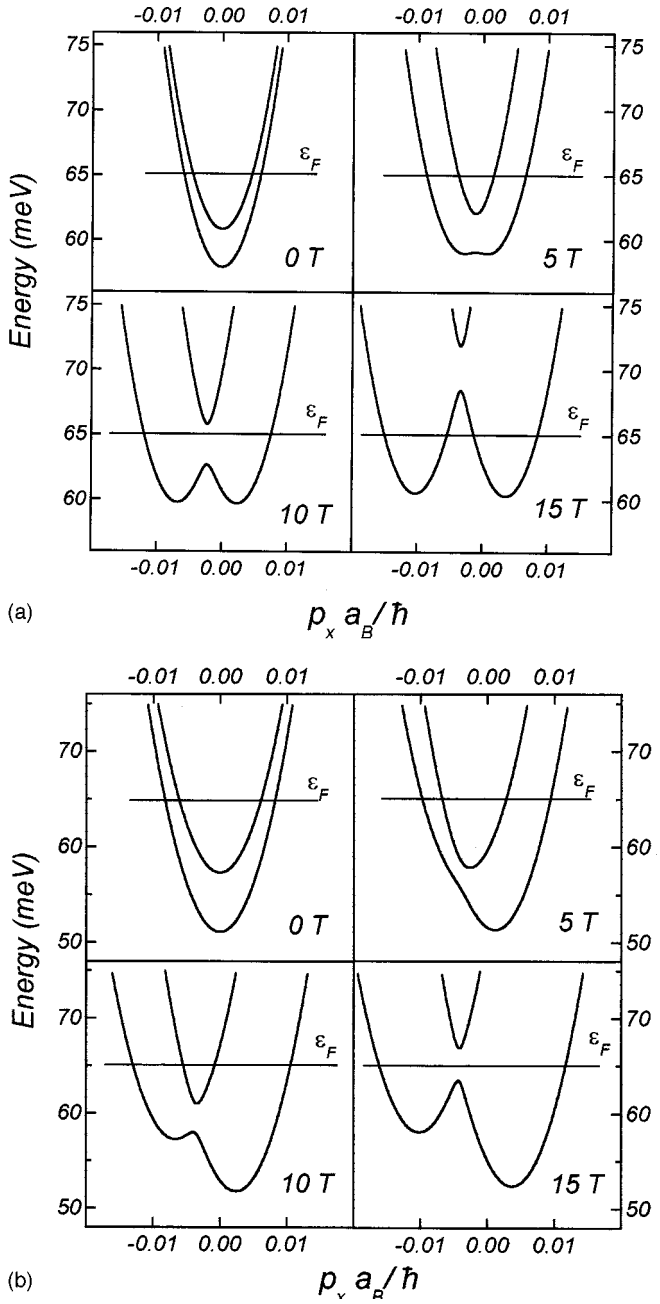

FIG. 2. Self-consistent dispersion laws, $E_{\pm p_x}$, for different magnetic fields $H=0$, 5, 10, and 15 T. Panel (a) shows symmetric DQW's without applied electric field, and panel (b) shows the same structure under transverse field $F_\perp=5$ KV/cm. (a_B is the Bohr radius).

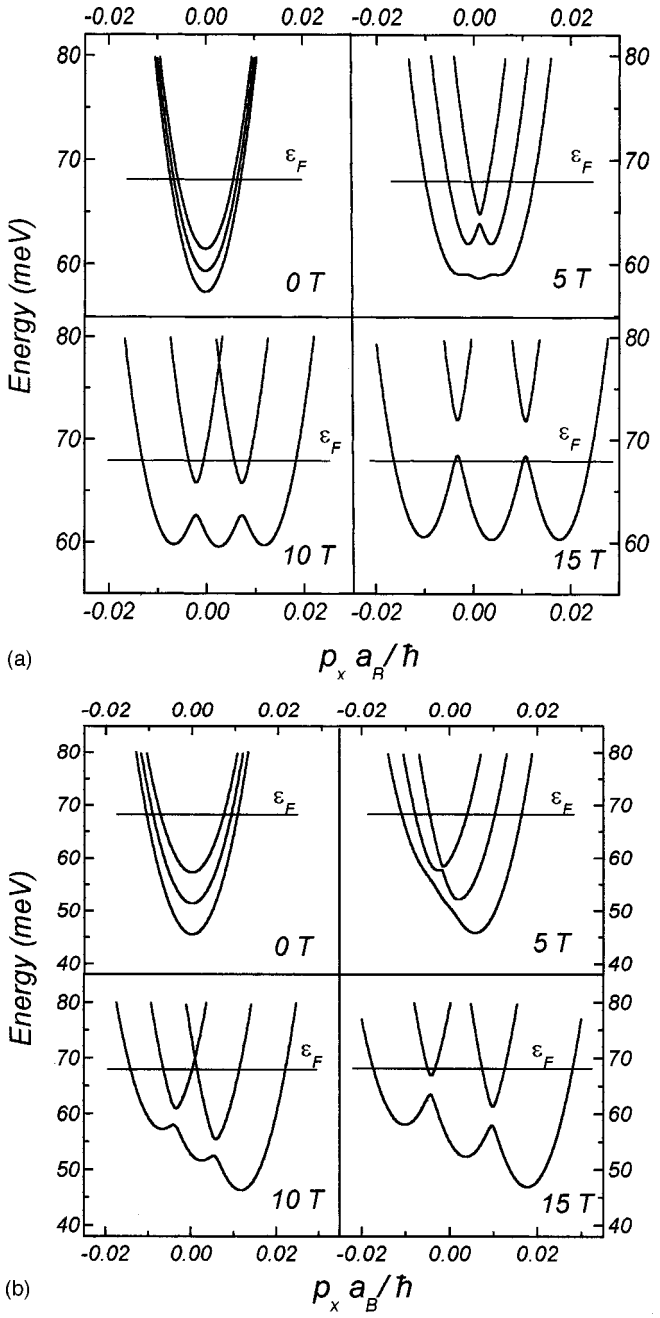

FIG. 3. The self-consistent dispersion laws for symmetric TQW's under the same magnetic fields as in Fig. 2. (a) $F_\perp=0$ KV/cm. (b) $F_\perp=5$ KV/cm. (a_B is the Bohr radius).

$$E_e=2\sum_j \int \frac{d\mathbf{p}}{(2\pi\hbar)^2}E_{j\mathbf{p}}\theta[\varepsilon_F-E_j(\mathbf{p})]$$

$$=\frac{2\rho_{2D}}{3\pi}\sum_j \int dp_x\sqrt{\frac{\varepsilon_F-E_{jp_x}}{2m}}(\varepsilon_F+2E_{jp_x}), \quad (14)$$

where we performed the integration over p_y in analogy with Eq. (10). Thus, in order to obtain the magnetization, we have to calculate the derivative of E_e using the dependence of ε_F from Eq. (11). Another phenomena is the interwell charge redistribution due to the modification of the wave function (2) under in-plane fields. The magnetoinduced voltage can be obtained from the total variation of the Hartree potential $U_{\rm sc}(z)$ across the heterostructure

$$\delta U=U_{\rm sc}(\infty)-U_{\rm sc}(\infty)_{|H=0} \quad (15)$$

and δU is found when solving the self-consistent eigenstate problem [see above Eqs. (1),(9)–(11)].

For the limit of weak tunneling, we neglect the anticrossing effect on the dispersion laws and the Fermi level remains the same for the overall QW structure (due to very slow interwell tunneling). After simple calculations of the integrals with the parabolic dispersion laws (4) we get $n_e\simeq\rho_{2D}\Sigma_j(\varepsilon_F-\varepsilon_{jH})\theta(\varepsilon_F-\varepsilon_{jH})$ and $E_e\simeq(\rho_{2D}/2)\Sigma_j(\varepsilon_F^2-\varepsilon_{jH}^2)\theta(\varepsilon_F-\varepsilon_{jH})$, where ε_{jH} takes into ac-

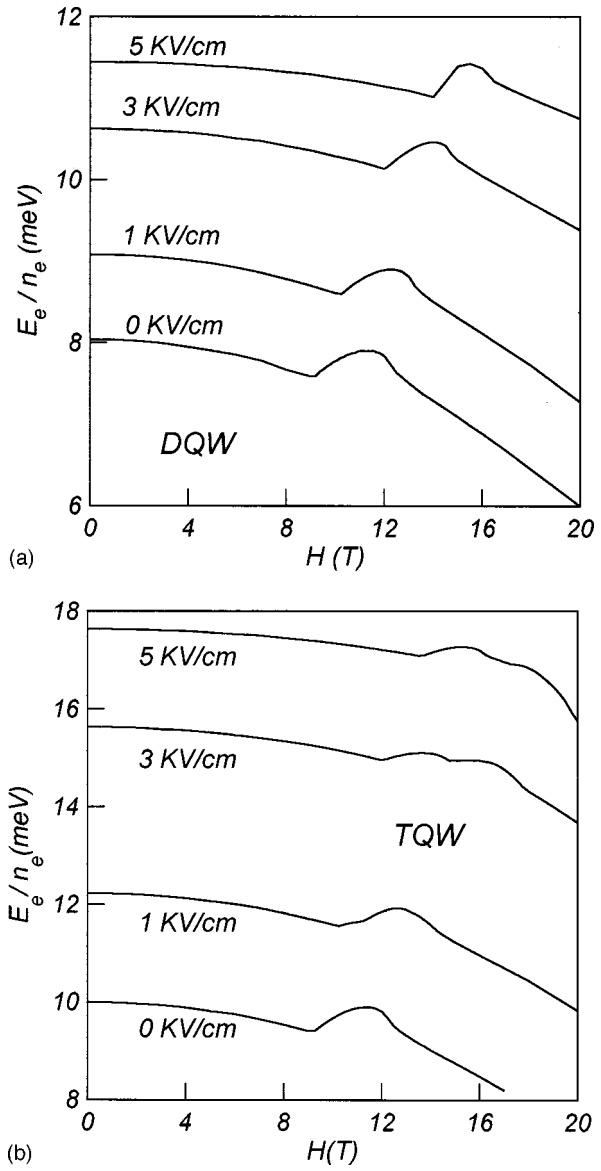

FIG. 4. The energy per electron, E_e/n_e, versus H for QW's under transverse fields $F_\perp = 0$, 1, 3 KV/cm, and 5 KV/cm. (a) DQW's. (b) TQW's.

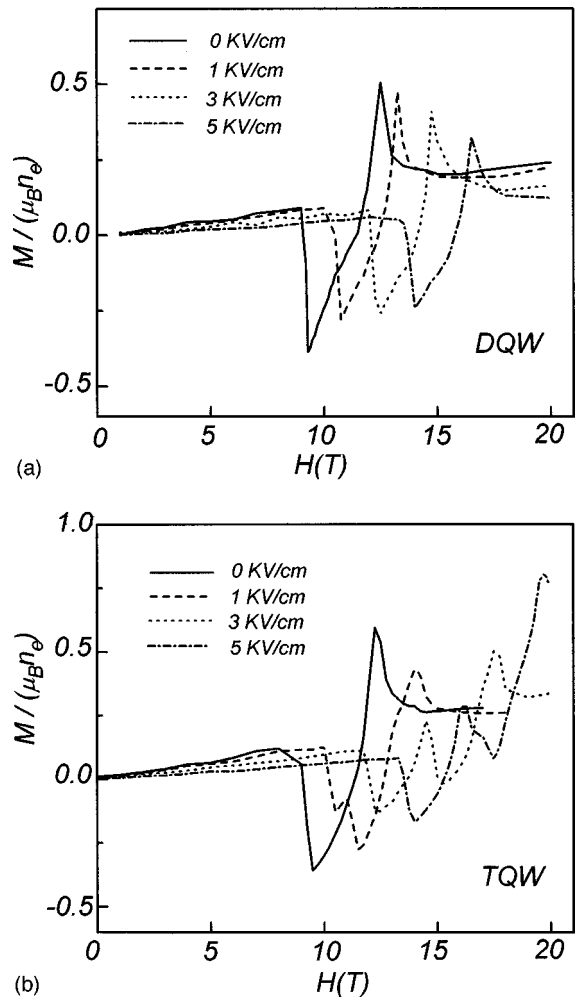

FIG. 5. Dimensionless magnetization per electron (μ_B is the Bohr magneton) versus magnetic field for $F_\perp = 0$, 1, 3 KV/cm, and 5 KV/cm. (a) DQW's. (b) TQW's.

count the proportional to H^2 contributions in Eq. (5). Then weak dependency $(E_e - E_{e|H=0}) \propto H^2$ (so that $M \propto H$) takes place for the case of DQW. Similar analysis for δU shows the dependency on H^2 also. However, these results are not true for the near anticrossing point regions and more complicated numerical consideration is necessary.

Thus, in order to perform the self-consistent calculations for M and δU for the magnetic-field range where the Fermi level intersects of the anticrossing region, we need to solve integrals (14) using the dispersion laws and ε_F from the solution of the self-consistent eigenstate problem; the transverse drop of potential give us δU.

Figures 4(a) and 4(b) show the expected parabolic relation $E_e(H)$, except for the above mentioned region (where the Fermi level passes through the small gap of an anticrossing point). In this region, a notable peak appears because of the electron energy increase. This maximum is shifted to higher magnetic fields when the electric field increases. The double hump (two maxima) observed in the $E_e(H)$ shape for TQW's case occurs because ε_F passes through the two possible anticrossings at slightly different magnetic-field intensities. As a consequence, dimensionless magnetization $M/(\mu_B n_e)$ versus H for TQW exhibits an additional structure at certain magnetic fields (μ_B is the Bohr magneton). We represent in Fig. 5 this dimensionless magnetization for symmetric DQW and TQW, and for different electric fields. As expected, the linear behavior of $M(H)$ is broken in the above-mentioned region. In spite of the changes in $M(H)$ are not too big because the heterostructures under consideration are weakly coupled, the typical values for $M/(\mu_B n_e)$ are comparable with experimental results.[15,16] It should be noticed that, for TQW's case, our calculations do not reach magnetic fields high enough to restore electron redistribution [linear behavior of $M(H)$] because the anticrossing energy splitting becomes broader as the *in-plane* magnetic field increases. As a consequence, the peculiarities region is dilated too.

Figures 6(a) and 6(b) show the DQW's magnetoinduced voltage $\delta U(H)$ and $\delta U(F_\perp)$ for different electric, $F_\perp$, and magnetic fields, H, respectively. $\delta U(H)$ decreases with increasing H to reach a minimum. This minimum nearly coincides with the Fermi level entrance into the anticrossing gap, marked by an arrow in figures. The other arrow indicates the

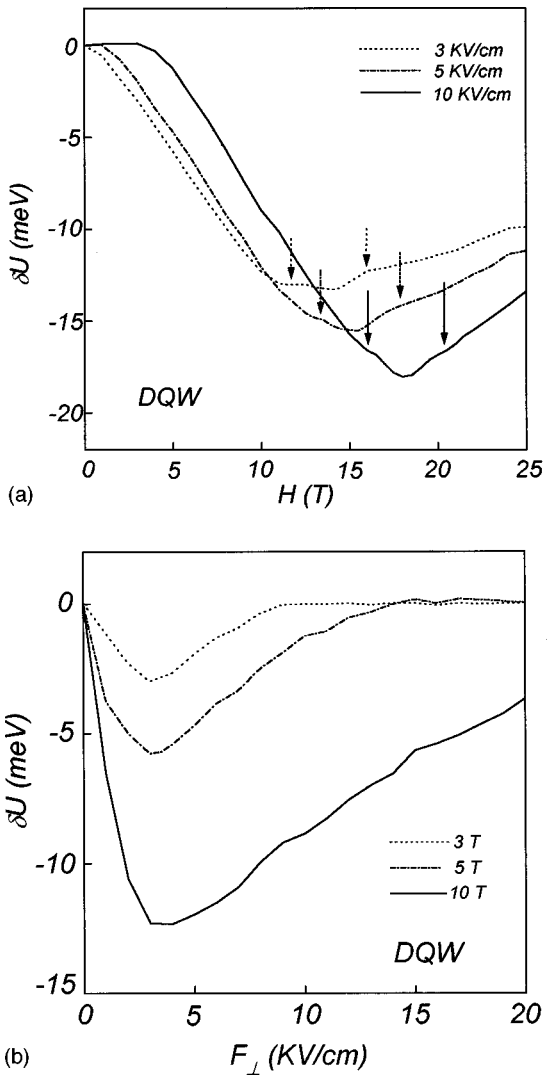

FIG. 6. (a) Magnetoinduced voltage versus magnetic field, $\delta U(H)$, for DQW's and for three different transverse electric fields, $F_\perp = 3$, 5, and 10 KV/cm. Arrows indicate the limits of the peculiarities region. (b) $\delta U(F_\perp)$ for DQW's and for three different magnetic fields, $H = 3$, 5, and 10 T.

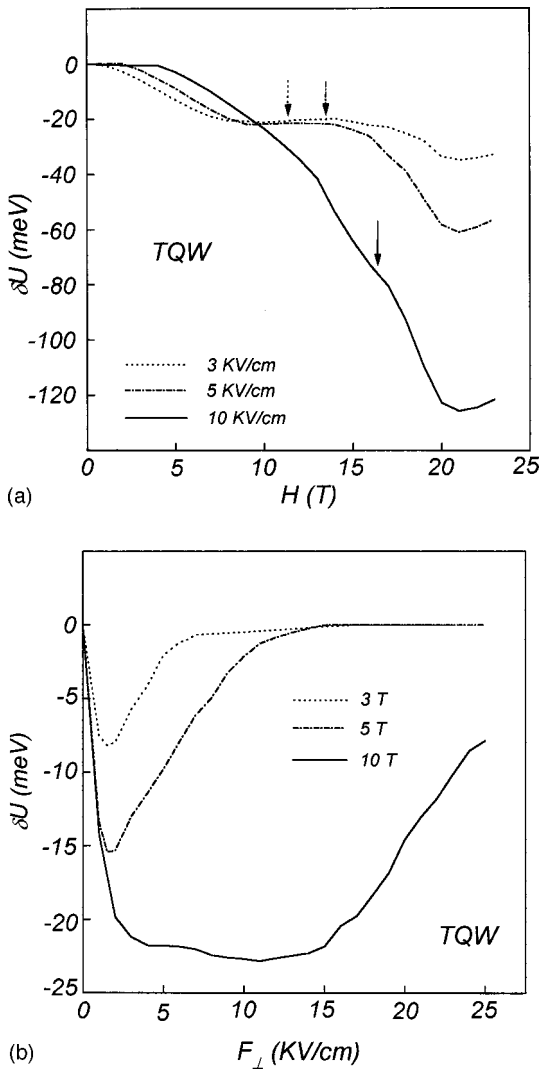

FIG. 7. (a) $\delta U(H)$ for TQW's, and for the same fixed transverse electric fields, $F_\perp$, as in Fig. 6. Arrows show the beginning of the peculiarities region. (b) $\delta U(F_\perp)$ for TQW's, and for fixed $H = 3$, 5, and 10 T.

exit of the Fermi level out this region. Then, magnetoinduced voltage grows to reach a constant value at higher magnetic fields. The case of $\delta U(F_\perp)$ is very different because ε_F never enters into the anticrossing gap for the fields under consideration. Once again a minimum occurs. Because peculiarities region is produced for in-plane magnetic fields beyond 10 T (DQW's) minimum positions do not depend on magnetic field and are located at a constant $F_\perp$ value around 3.5 KV/cm. An analogous behavior occurs for TQW's [Figs. 7(a) and 7(b)]. In the last case magnetoinduced voltage is one order of magnitude bigger than for the DQW's one. $\delta U(F_\perp)$ minima are close to 2 KV/cm for TQW's case, except for $H = 10$ T, where a flat magnetoinduced region occurs before electron redistribution. Again, very strong-magnetic fields are needed to reach the electron redistribution equilibrium across the structure.

IV. CONCLUDING REMARKS

Using both simple analytical considerations and numerical calculations, we have taken into account the peculiarities of electron energy spectra in tunnel-coupled structures and the modifications of their properties under in-plane magnetic field. We have proved that peculiarities of the energy spectra near double- and triple-cross point of the dispersion branches may be investigated to study collisionless characteristics as the magnetization and the magnetoinduced transverse voltage. Results show that magnetization under in-plane magnetic fields and induced voltage change essentially for the fields at which the Fermi level intersects the anticrossing region in DQW's or TQW's. To the best of our knowledge, both theoretical and experimental magnetization for any 2D system under *in-plane* magnetic fields are not available at the present.

Let us discuss the approximations used above. The self-consistent calculations based on the Hamiltonian (1) with the potential (9) did not take into account the exchange-correlation corrections, which are essential for structures with low-sheet densities[18] ($<10^{10}\,\mathrm{cm}^{-2}$) far from the one used in this paper. We neglect also the scattering effect on the energy spectra, which leads to the broadening of the near cross-point peculiarities. Since these cross points take place

at strong-magnetic fields (above 8 T in Figs. 2 and 3 where the level splitting is about 4 meV) this broadening is weak enough. We consider here the case with fixed electron density n_e in the structure; another variant may be realized if the structure under consideration is coupled with the doped bulk region when the chemical potential is fixed and n_e is changed under H and $F_\perp$ variations. For such a case, M and δU are of the order of the values calculated above but dependencies should be different (in this paper, we did not calculate the magnetocapacitance, which depends on the profile of doping).

In conclusion, in this paper we suggest that the experimental study of the modulation of equilibrium properties by the in-plane magnetic field would be a direct method to study the level anticrossing phenomena in tunnel-coupled structures.

ACKNOWLEDGMENT

This work has been supported in part by Gobierno Autónomo de Canarias, Consejería de Educación, Cultura y Deportes.

*Electronic address: ajhernan@ull.es

[1] J. A. Simmons, S. K. Lyo, N. E. Harf, and J. F. Klem, Phys. Rev. Lett. **73**, 2256 (1994).

[2] A. Kurobe, I. M. Castleton, E. H. Linfield, M. P. Grimshaw, K. M. Brown, D. A. Ritchie, M. Pepper, and G. A. C. Jones, Phys. Rev. B **50**, 4889 (1994).

[3] Y. Ohno, H. Sakaki, and M. Tsuchiya, Phys. Rev. B **49**, 11 492 (1994).

[4] Y. Berk, A. Kamenev, A. Palevski, L. N. Pfeifer, and K. W. West, Phys. Rev. B **51**, 2604 (1995).

[5] I. S. Millard, N. K. Patel, C. L. Foden, M. Y. Simmons, D. A. Ritchie, G. A. C. Jones, and M. Pepper, Phys. Rev. B **55**, R13 401 (1997); N. E. Harff, J. A. Simmons, S. K. Luo, J. F. Klem, G. S. Boebinger, L. N. Pfeiffer, and K. W. West, *ibid.* **55**, R13 405 (1997).

[6] T. Jungwirth, T. S. Lay, L. Smrcka, and M. Shayegan, Phys. Rev. B **56**, 1029 (1997).

[7] T. S. Lay, X. Ying, and M. Shayegan, Phys. Rev. B **52**, R5511 (1995).

[8] O. E. Raichev and F. T. Vasko, Phys. Rev. B **53**, 1522 (1996); F. T. Vasko and O. E. Raichev, *ibid.* **52**, 16 349 (1994).

[9] Y. Kim, C. H. Perry, D. G. Rickel, J. A. Simmons, J. F. Klem, and E. D. Jones, in *Proceedings of the 23rd International Conference on the Physics of Semiconductors*, edited by M. Scheffler and R. Zimmermann (World Scientific, Singapore, 1996), p. 1859.

[10] N. K. Patel, A. Kurobe, I. M. Castelton, E. H. Linfield, K. M. Brown, M. P. Grimshaw, D. A. Ritchie, G. A. C. Jones, and M. Pepper, Semicond. Sci. Technol. **11**, 703 (1996).

[11] S. K. Lyo, Phys. Rev. B **50**, 4965 (1994).

[12] S. K. Lyo, D. Huang, J. A. Simmons, and N. E. Harff, in *Proceedings of the 24th International Conference on the Physics of Semiconductors, Jerusalem, 1998*, edited by D. Gershoni (World Scientific, Singapore, 1999); D. Huang and S. K. Lyo, Phys. Rev. B **59**, 7600 (1999).

[13] D. D. Arnone, T. P. Marlow, C. L. Foden, E. H. Linfield, D. A. Ritchie, and M. Pepper, Phys. Rev. B **56**, R4340 (1997).

[14] A. Hernández-Cabrera and A. Ramos, Superlattices Microstruct. **23**, 521 (1998).

[15] J. P. Eisenstein, H. L. Stormer, V. Narayanamurti, A. Y. Cho, A. C. Gossard, and C. W. Tu, Phys. Rev. Lett. **55**, 875 (1985); S. A. J. Wiegers, M. Specht, L. P. Levy, M. Y. Simmons, D. A. Ritchie, A. Cavanna, B. Etienne, G. Martinez, and P. Wyder, *ibid.* **79**, 3238 (1997).

[16] I. Meinel, D. Grundler, S. Bargstadt-Franke, C. Heyn, and D. Heitmann, Appl. Phys. Lett. **70**, 3305 (1997).

[17] O. Z. Olendskii, Fiz. Tverd. Tela **34**, 3087 (1992) [Sov. Phys. Solid State **34**, 1653 (1992)].

[18] P. P. Ruden and Z. Wu, Appl. Phys. Lett. **59**, 2165 (1991); F. A. Reboredo and C. R. Proetto, Phys. Rev. Lett. **79**, 463 (1997); R. J. Radtke, S. Das Sarma, and A. H. MacDonald, Phys. Rev. B **57**, 2342 (1998).